Differential Perturbation of Intersubunit and Interdomain Communications by Glycine 141 Mutation in *Escherichia coli* CRP†

Xiaodong Cheng‡ and J. Ching Lee*

Department of Human Biological Chemistry and Genetics, The University of Texas Medical Branch at Galveston, Galveston, Texas 77555-1055

Received August 6, 1997; Revised Manuscript Received October 27, 1997⊗

ABSTRACT: Upon binding of cAMP, concomitant changes in CRP structure across the subunit and domain interfaces are observed. In order to identify the structural elements involved in the coupling of interfacial interactions, structural perturbation was introduced at residue 141 by site-directed mutagenesis. Thermodynamic parameters defining protein stability, cAMP binding, and subunit assembly of the mutant were determined. Conformational changes probed by proteolytic digestion and fluorescence signal reported by the fluorescein-labeled C178 lead to a dissection of the contribution of the intersubunit and interdomain interactions, respectively, in the cAMP-modulated DNA binding of CRP. In the absence of cAMP, mutant G141Q is sensitive to protease attack at the subunit interface, an established property of wild type CRP observed only in the presence of cAMP. Although the G141Q mutant assumes a subunit alignment similar to that of the activated CRP, this mutant absolutely requires cyclic nucleotide for specific DNA interaction. Monitoring the fluorescence probe attached to the C-terminal DNA binding domain of the G141Q mutant showed that the DNA binding domain responds quantitatively to the binding of cyclic nucleotide to the N-terminal domain. This result suggests that domain reorientation is a required structural change in addition to subunit alignment. In summary, mutation at G141 has differentially perturbed the communication network which involves the interfacial interactions between subunits and domains. The G141Q CRP mutant assumes a conformation that partially resembles the active form represented by the observed subunit realignment, but complete activation of the mutant requires binding of cyclic nucleotide which induces the reorientation of domains. Furthermore, the G → Q mutation leads to a loss in the discriminatory power of CRP for only cAMP. Other cyclic nucleotides are capable of activating this mutant.

Control of gene expression is modulated by complex interactions made by specific DNA sequences and regulatory proteins. Communication among these components is mediated by the precise signals transmitted by allosteric conformational changes accompanying each interaction. cAMP receptor protein (CRP[1]) is a key regulatory protein that controls the expression of many genes involved in different cellular functions in *Escherichia coli* (*1*−*3*). CRP is a homodimeric protein. Each subunit is composed of two domains connected by a hinge region. The small carboxyl-terminal domain contains a helix-turn-helix DNA binding motif. The large amino-terminal domain is responsible for cyclic nucleotide binding (*4*).

In its ligand-free or fully liganded states, CRP exhibits low affinities to specific DNA sequences, while the mono-liganded CRP, CRP−$cAMP_1$ complex, binds to specific DNA sequences with high affinities (*5*−*8*). This allows CRP to turn on or off a particular gene at a specific cAMP concentration window in response to the change of environment. When bound to DNA, CRP−$cAMP_1$ complex induces structural distortions in the DNA (*9*−*11*) and makes contacts with RNA polymerase (*9, 12*−*17*) and eventually leads to the activation of a specific gene.

A fundamental issue concerning the molecular mechanism of CRP activation is: How does cAMP activate CRP and what are the allosteric conformational changes in CRP induced by the binding of cAMP? Answers to these questions remain elusive, in part because the only CRP crystalline structure available is that of the doubly liganded CRP, CRP−$cAMP_2$, which has been shown to exhibit low affinity for specific DNA in solution (*6*−*8*). At present, two models for the cAMP-induced CRP activation have been proposed in the literature. In the first model the conformational effects induced by cAMP are considered to be transmitted mainly through the monomer units from the cAMP binding domain to the DNA binding domain containing the distal F helix which is responsible for contacting DNA (*18*−*20*). The evidence sited in support for this model comes from studies of a class of CRP mutant, CRP*, which can activate CRP-dependent transcription *in vivo* in the absence of exogenous cAMP in cya^- strains (*21*−*28*). It was assumed that these CRP* mutants are already in an

† Supported by NIH Grant GM-45579 and Robert A. Welch Foundation Grants H-0013 and H-1238.

‡ Present address: Department of Chemistry and Biochemistry, The University of California, San Diego, La Jolla, CA 92093-0654.

⊗ Abstract published in *Advance ACS Abstracts,* December 15, 1997.

[1] Abbreviations used: ANS, 8-anilino-1-naphthalenesulfonic acid; CD, circular dichroism; CRP, cAMP receptor protein; FITC, fluorescein 5-isothiocyanate; GuHCl, guanidine hydrochloride; IAF, iodoacetamidofluorescein; buffer A, 50 mM Tris, 0.1 M KCl, 1 mM EDTA at pH 7.8.

S0006-2960(97)01945-4 CCC: $15.00
Published on Web 01/06/1998

FIGURE 1: Structure of CRP. A ribbon representation of CRP dimer with one subunit in white and another subunit in gray. The location of residues Gly 141, Cys 178, the F-helix (the DNA recognition helix), and the C-helices at the dimer interface are marked. This structure was generated using coordinates from Weber and Steitz (1987).

active conformation, thus no additional conformational changes induced by cAMP binding are required (*18*−*21, 29*). Since the sites of mutation in most CRP* mutants are located in the D helix near the hinge region, it has been proposed that replacing the native amino acid residues with bulkier side chains at these locations introduces a steric repulsion with the nearby F helix which is then appropriately positioned to interact with DNA (*19, 20*). The central feature of the second model requires an overall realignment of the two subunits and rearrangement of the two domains within each subunit upon binding of cAMP to the CRP. These structural changes lead to the positioning of the DNA recognition F helix for DNA binding. The cited evidence in support of this model is that cAMP binds to the subunit interface of the CRP dimer and interacts with both subunits in the CRP crystal structure (*4, 30*) and that the activation of CRP require only one cAMP molecule (*5*−*8*). Regardless of the model for communication pathway, concomitant structural changes in the subunit and domain interfaces are observed (*6*). Thus, which structure element is responsible for the coupling? What is the consequence of uncoupling the interfacial interactions?

To address these questions, a strategy was adopted to study CRP mutants with different phenotypic characteristics. In this study, biochemical and biophysical properties of a CRP* mutant, G141Q CRP, were monitored, with special attention to the subunit and domain interactions. The choice of this mutant is based on the intriguing observation from this laboratory that *in vitro* binding of this mutant to specific DNA sequence absolutely requires exogenous cyclic nucleotides (*31*). The location of residue 141 in the CRP homodimer is shown in Figure 1. Results from such studies allow a quantitative dissection of the partial reactions which constitute the CRP activation process.

MATERIALS

Chymotrypsin A and cGMP were purchased from Boehringer Mannheim. Altered Sites *in vitro* Mutagenesis System was obtained from Promega, and Sequenase version 2.0 was from United States Biochemical Corporation, Inc. Subtilisin (protease type XXVII) and cAMP were purchased from Sigma. Ultrapure guanidine HCl was a product of ICN Biochemical. FITC and IAF were purchased from Molecular Probes. Oligonucleotides were synthesized by Genosys. ANS (Kodak Lab) was further purified as described by York et al. (*32*). Restriction Endonucleases were from Promega, Gibco BRL, United States Biochemical Corporation, Inc., or Boehringer Mannheim.

E. coli K-12 Δ H1 (*F*$^-$, Δ(*bio*$^-$, *uvr*B), lacZam, λ, Nam7, Nam53, cI857, Δ H1(cro-F-A-J-b2)) and K-12 BR469 (Δ(*lac*) Δ(*gal*(attL λ G) J$^+$-lacZ$^+_{w205}$ trpAB$^+_{11/14\ 1c}$::redB λ cI$^+$ T11 E$^+$ Δ(G attR) bio uvrB) thi strA) were from American Type Culture Collection. *E. coli* CA8445 (HfrH Δcrp-45 Δcya-854 strA thi) (*33*) and PRK248cI^{ts} (*34*) which encodes a temperature sensitive λ cI repressor were kindly provided by Dr. Peterkofsky of the National Heart, Lung and Blood Institute. pPLcCRP1, a pPLc28 derivative that contains the wild type *crp* gene under the control of λP_L promoter, was a gift from Drs. Gronenborn and Clore of NIH (*35*).

METHODS

All experiments, except specifically indicated, were conducted in buffer A. The concentration of protein, cAMP, and fluorescence probes was determined by absorption spectroscopy using the following absorption coefficients: 20 400 M^{-1} cm^{-1} at 278 nm for CRP monomer (*36*); 14 650 M^{-1} cm^{-1} at 259 nm for cAMP (*37*); 6420 M^{-1} cm^{-1} at 351 nm for ANS (*38*); 70 800 M^{-1} cm^{-1} at 494 nm for fluorescein (*39*).

Site-Directed Mutagenesis. Point mutation of glycine to glutamine at residue 141 was generated as previously described (*39, 40*).

Lac Operon Activation in Vivo. To test the effects of mutation on the *lac* operon expression, *E. coli* CA8445/pPRK248cI^{ts}, transformed with plasmid pPLc28 that encoded the appropriate *crp* mutant gene, was streaked on MacConkey lactose indicator plates in the absence or presence of 0.5 mM cAMP or cGMP. The plates were incubated at 37 °C overnight. The scoring of fermentation response of the mutant was based upon the color of the colonies on the plates. A CRP* phenotype is defined as an amino acid substitution that shows purple colonies on MacConkey lactose plate (*Lac*$^+$) in the absence of external cAMP or in the presence of cGMP.

Protein Purification. Wild type CRP was purified from temperature-induced *E. coli* K12 ΔH1/pPLcCRP1 cells grown in LB. For isolation of mutant CRP, plasmid pPLc28 encoding the appropriate mutant *crp* gene was first introduced into *E. coli* CA8445/pPRK248cI^{ts}. The recombinant bacteria were then grown in LB medium at 28 °C. When the optical density of the bacterial culture reached 0.6−0.8 at 600 nm, the incubation temperature was shifted to 42 °C for another 12 h to induce the expression of the mutant CRP protein. Mutant CRP was isolated to more than 95% pure

as judged by SDS-PAGE using a similar protocol for wild type CRP purification (*6*, *41*).

Circular Dichroism. CD spectra of the wild type CRP and mutants were measured with an Aviv 62 DS circular dichroism spectrometer. To acquire a full range of near- and far-UV CD spectrum, fused quartz cuvettes with pathlengths of 0.01 (220−190 nm), 0.1 (270−200 nm), and 1 cm (360−240 nm) and protein solutions with concentration around 1 mg/mL were used. Each spectrum was recorded with a 0.5 nm increment and 1 s interval. For each sample five repetitive scans were obtained and averaged.

Sedimentation Equilibrium. The quaternary structure of CRP was monitored by sedimentation equilibrium as previously described (*42*). Experiments were conducted in a Beckman-Spinco Model E analytical ultracentrifuge equipped with a photoelectric scanner, an electronic speed control, and an RTIC temperature control. The high-speed, meniscus-depletion procedure was employed (*43*). The loading CRP concentrations were between 0.2 and 0.4 mg/mL. Sedimentation data were acquired (10 scans) and then averaged after reaching equilibrium. Density of the solution was determined with a Mettler-Paar Precision DMA-02D density meter. Values of the partial specific volume of the wild type and mutant CRPs in native buffer and 6.0 M GuHCl were calculated on the basis of the amino acid composition of CRP (*44*, *45*) using the procedures of Cohn and Edsall (*46*) and Lee and Timasheff (*47*), respectively.

Sedimentation equilibrium data were fit by nonlinear least squares to a model of dimer assembly according to

$$C = \Delta C + \exp[\ln C_0 \,\sigma(r^2/2 - r_0^2/2)] + \exp[2 \ln C_0 + 2\sigma(r^2/2 - r_0^2/2) + \ln K] \quad (1)$$

where C is the CRP concentration observed at radial position r, ΔC is the base line offset, C_0 is the concentration of CRP at the meniscus (r_0), K is the dimer equilibrium association constant, and σ is the reduced molecular weight given by $\sigma = M_r(1 - \bar{v}\rho)\,\omega^2/2RT$, where M_r is the monomer molecular weight, $\bar{v}$ is the partial specific volume, ρ is the solution density, ω is the angular velocity, and R and T are the gas constant and the temperature in Kelvin, respectively.

Denaturation of CRP. Studies of GuHCl-induced denaturation of CRP were carried out by a published procedure (*42*). Briefly, the denaturation equilibrium of CRP can be described by a three-state model

$$N_2 \overset{K_d}{\rightleftharpoons} 2N \overset{K_u}{\rightleftharpoons} 2U \quad (2)$$

in which N_2, N, and U are folded dimer, folded monomer, and unfolded monomer of CRP, respectively. K_d and K_u are the equilibrium constants of dissociation and unfolding, respectively. Unlike the wild type CRP, mutant G141Q exhibits a weakened subunit association which leads to a complete uncoupling of the dimer dissociation and monomer unfolding. Therefore, these two processes can be studied separately. Subunit association of G141Q was measured by sedimentation equilibrium as described above. CRP unfolding was monitored by fluorescence anisotropy at 280 and 345 nm, the excitation and emission wavelengths, respectively.

To determine the equilibrium constant upon unfolding, the fraction of CRP protein that is in the folded state, f, was calculated by

$$f = F(\epsilon - \epsilon_{unfolded})/(\epsilon_{folded} - \epsilon + F\epsilon - F\epsilon_{unfolded}) \quad (3)$$

where ϵ, ϵ_{folded}, and $\epsilon_{unfolded}$ represent the measured fluorescence anisotropy signal of the protein sample and values of fluorescence anisotropy of folded and unfolded CRP at a given GuHCl concentration. F, the correction factor, is the ratio of the fluorescence intensity of folded to that of unfolded G141Q monomer (*48*). ϵ_{folded} and $\epsilon_{unfolded}$ at the unfolding transition zone were derived by linear extrapolation of the measured signals at the predenaturation and postdenaturation zones, respectively.

Once f was determined, the equivalent K_u at different GuHCl concentrations can be calculated as

$$K_u = \frac{[U]}{[N]} = \frac{1 - f}{f} \quad (4)$$

Consequently, K_u values were converted to ΔG_u by $\Delta G_u = -RT \ln K_u$ and ΔG_u^0, the free energy of unfolding in the absence of denaturant, was subsequently determined by linear extrapolation of ΔG_u to zero denaturant concentration.

Fluorescence Labeling of CRP. IAF modification of the wild type and mutant CRPs was carried out in 50 mM Tris, 0.3 M KCl, 1 mM EDTA, pH 7.8 in the dark. CRP (1.1 mg/mL) was modified by 0.5 mM IAF at 4 °C overnight for the wild type CRP and 30−45 min at room temperature for G141Q. FITC modification was performed in 50 mM Tris, 0.2 M KCl, 1 mM EDTA, 1 mM DTT at pH 8.5 with a CRP concentration of 10 μM and a molar ratio of 1:35 for protein to probe for 3 h at room temperature. Fluorescently labeled CRP was purified by Sephadex G-25 spin columns and dialyzed extensively against buffer A. The extent of modification was determined as previously described (*11*, *49*).

cAMP Binding Assays. cAMP binding to CRP was measured by monitoring the intrinsic tryptophan fluorescence of CRP (λ_{ex} = 300 or 305 nm, λ_{em} = 345 nm), or the quenching of ANS-CRP fluorescence (λ_{ex} = 375 nm, λ_{em} = 480 nm), or the fluorescence signal change of the CRP-IAF (λ_{ex} = 495 nm, λ_{em} = 520 nm). The basic protocol employed has been previously described (*6*) with a minor modification (*40*). All fluorescence measurements were performed with a SLM 8000C spectrofluorometer with a temperature-controlled water bath at 25 °C. Emission spectra were collected with excitation and emission polarizers set at 90° and 54.7° (magic angle), respectively. If necessary, titration points were corrected for dilution and inner filter effects using the following formula (*50*):

$$F_{i,cor} = (F_i - B_i)\,(V_i/V_0)\,\frac{P_0 + \Delta A}{P_0}\,\frac{1 - 10^{-P_0}}{1 - 10^{-(P_0 + \Delta A)}} \quad (5)$$

where $F_{i,cor}$, F_i, B_i, and V_i are the corrected values of the fluorescence intensity, measured fluorescence intensity, background intensity, and volume of the sample at a given point of titration i, respectively. P_0 and ΔA denote the initial sample absorption and the absorption change introduced by the titration procedure.

CRP exists as a dimer in solution and can bind to two molecules of cAMP per dimer. Binding of cAMP to CRP can be described in accordance with the following equations:

$$\mathrm{CRP} + \mathrm{cAMP} \overset{K_1}{\rightleftharpoons} \mathrm{CRP{-}cAMP_1} \tag{6}$$

$$\mathrm{CRP} + 2\mathrm{cAMP} \overset{K_2}{\rightleftharpoons} \mathrm{CRP{-}cAMP_2} \tag{7}$$

with $K_1 = [\mathrm{CRP{-}cAMP_1}]/[\mathrm{CRP}][\mathrm{cAMP}]$ and $K_2 = [\mathrm{CRP{-}cAMP_2}]/[\mathrm{CRP}][\mathrm{cAMP}]^2$.

Therefore, all cyclic nucleotide binding data in this study can be fitted to the following equation by a nonlinear least-squares procedure to yield thermodynamic parameters: K_1, K_2, Δ_1, and Δ_2 (*6*)

$$\Delta_{\mathrm{obs}} = \frac{\Delta_1 K_1[\mathrm{cAMP}] + \Delta_2 K_2[\mathrm{cAMP}]^2}{1 + K_1[\mathrm{cAMP}] + K_2[\mathrm{cAMP}]^2} \tag{8}$$

where Δ_{obs}, Δ_1, and Δ_2 are the values of change in a measured property, normalized values of change in the property in going from the free CRP to $\mathrm{CRP{-}cAMP_1}$ and $\mathrm{CRP{-}cAMP_2}$, respectively, K_1 and K_2 are Adair constants for the formation of $\mathrm{CRP{-}cAMP_1}$ and $\mathrm{CRP{-}cAMP_2}$, and [cAMP] is the free cAMP concentration.

cAMP Binding to CRP Monomer. To estimate the binding constant of cAMP to G141Q monomer, the apparent dimer association constant of G141Q-FTIC was monitored by sedimentation equilibrium at 495 nm as a function of cAMP. The scheme of CRP dimer association linked to the cAMP binding can be described as follows:

$$\begin{array}{ccc} 2\mathrm{P} + 2\mathrm{cAMP} & \overset{K_a}{\rightleftharpoons} & \mathrm{P_2} + 2\mathrm{cAMP} \\ \Big\Updownarrow K_m & & \Big\Updownarrow K_{b1} \\ \mathrm{P{-}cAMP_1} + \mathrm{P} + \mathrm{cAMP} & \overset{K_{a1}}{\rightleftharpoons} & \mathrm{P_2{-}cAMP_1} + \mathrm{cAMP} \\ \Big\Updownarrow K_m & & \Big\Updownarrow K_{b2} \\ 2\mathrm{P{-}cAMP_1} & \overset{K_{a2}}{\rightleftharpoons} & \mathrm{P_2{-}cAMP_2} \end{array}$$

Therefore, the apparent dimer association of G141Q-FTIC in the presence of cAMP can be expressed as

$$K_{\mathrm{a,app}} = \frac{\sum[\mathrm{P_2}]}{(\sum[\mathrm{P}])^2} = \frac{[P_2] + [P_2 - \mathrm{cAMP_1}] + [P_2{-}\mathrm{cAMP_2}]}{([P] + [P{-}\mathrm{cAMP_1}])^2} \tag{9}$$

Equation 9 can be further simplified as

$$K_{\mathrm{a,app}} = K_{\mathrm{a}} \frac{1 + K_{\mathrm{b1}}[\mathrm{cAMP}] + K_{\mathrm{b1}}K_{\mathrm{b2}}[\mathrm{cAMP}]^2}{(1 + K_{\mathrm{m}}[\mathrm{cAMP}])^2} \tag{10}$$

where $K_{\mathrm{m}} = [\mathrm{P{-}cAMP_1}]/[\mathrm{P}][\mathrm{cAMP}]$, $K_{\mathrm{b1}} = [\mathrm{P_2{-}cAMP_1}]/[\mathrm{P_2}][\mathrm{cAMP}]$, $K_{\mathrm{b2}} = [\mathrm{P_2{-}cAMP_2}]/[\mathrm{P_2{-}cAMP_1}]\,[\mathrm{cAMP}]$, and $K_{\mathrm{a}} = [\mathrm{P_2}]/[\mathrm{P}]^2$. Since K_{b1} and K_{b2} can be independently determined by cAMP binding assay, K_{m} can be estimated by measuring $K_{\mathrm{a,app}}$ as a function of cAMP concentration.

RESULTS

Mutagenesis. Point mutant G141Q was generated by site-directed mutagenesis and has been described previously (*40, 41*). G141Q, when expressed in *E. coli* CA8445/pPRK248cI^{ts}, a *crp*$^-$/*cya*$^-$ strain, displayed purple colonies on the MacConkey plate in the absence of exogenous cAMP or in the presence of cGMP as reported earlier (*19, 51*). Thus this mutant is characterized by a CRP* phenotype.

Structural Integrity of the CRP Mutant. Near and far-UV CD spectra of G141Q show no significant difference from that of the wild type (Figure 2). This result indicates that introduction of mutation G141Q into CRP does not affect the secondary and tertiary structure of CRP.

Subunit Association. The effect of mutation on the quaternary structure of CRP is probed by monitoring the energetics of dimer formation of the mutant. The propensity for the mutant to dissociate was monitored by sedimentation equilibrium. The sedimentation profiles of mutant G141Q and wild type CRP in the presence of 2.25 M GuHCl were analyzed. Wild type CRP exhibits apparent molecular weight that is between that of monomeric and dimeric CRP. In contrast, a much smaller apparent molecular weight for G141Q was obtained relative to wild type CRP, indicating a greater tendency for G141Q to dissociate at the same denaturant concentration. A systematic study of mutant G141Q as a function of GuHCl concentration was initiated to determine the dimer dissociation constant. The experimental data were then analyzed to estimate the apparent dimer association constants, $K_{\mathrm{a,app}}$, at individual GuHCl concentrations using the program NONLIN (*52*), as shown in Figure 3. A plot of ln $K_{\mathrm{a,app}}$ versus GuHCl concentration displays an apparent linear relationship. Extrapolation of the data to zero concentration of GuHCl yields a value of the dimer association constant for G141Q in buffer, as shown in Figure 3B. This value of 7.1×10^6 M^{-1} is very close to the actual measured value in the absence of GuHCl by sedimentation equilibrium. This identity of K_{a} values demonstrates that the linear extrapolation method used in this and previous studies (*40, 42*) is a thermodynamically valid approach for studying dissociation of tightly associated oligomers that are practically very difficulty to measure using conventional methods.

cAMP Binding. Interaction of cAMP with mutant G141Q displayed a biphasic pattern reflecting consecutive binding of two cAMP molecules to each CRP dimer regardless of the probe employed, be it ANS or intrinsic tryptophan, as shown in Figures 4A and 4B, respectively. However, the response of G141Q to increasing cAMP concentration as monitored by intrinsic tryptophan fluorescence which is located in the cAMP binding domain is rather different from that of the wild type. The change in fluorescence signal induced by cAMP binding to G141Q at low ligand concentration is pronounced, amounting to approximately 50% of the total change, as shown in Figure 4B. The magnitude of change is significantly higher than the 5% change observed in wild type CRP (*6*). A perturbation of tryptophan fluorescence intensity upon binding of the first cAMP to G141Q implies that the protein undergoes a structural change and the larger magnitude of change implies that the conformational state of the ligand free G141Q assumes a conformation that is significantly different from that of the free wild type CRP. Hence, the functional mechanism of CRP* is more complicated than it was originally proposed; namely, CRP* assumes a functional state that is the same as the $\mathrm{CRP{-}cAMP_1}$ complex so it can activate gene expression in

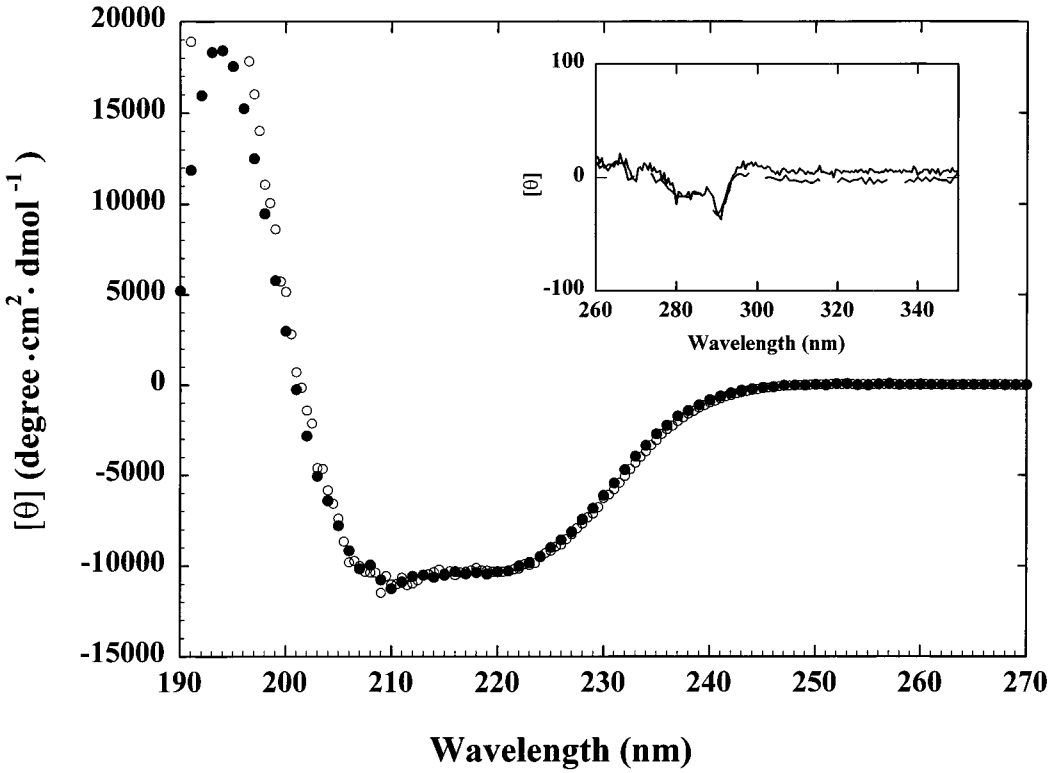

FIGURE 2: CD spectra of the G141Q (○) and wild type CRP (●) in buffer A. Inset: CD signals of the wild type CRP (long dashed line) and G141Q (solid line) at the near-UV region. The axes of the inset and the figure are the same.

Table 1: Summary of Fitted Parameters for Cyclic Nucleotide Binding to G141Q− CRP

		K_1 (M^{-1})	k_1 (M^{-1})	K_2 (M^{-2})	k_2 (M^{-1})	k_1/k_2
wild type	average[a]		2.5×10^4		1.0×10^3	25
G141Q	tryptophan	1.1 (1.0, 1.3)[b] $\times 10^5$	5.6×10^4	3.2 (2.3, 4.9) $\times 10^8$	5.7×10^3	
	ANS	7.3 (7.3, 7.3) $\times 10^4$	3.7×10^4	4.4 (4.4, 4.4) $\times 10^7$	1.2×10^3	26
	fluorescein	2.0 (1.8, 2.1) $\times 10^5$	1.0×10^5	6.6 (5.6, 7.4) $\times 10^7$	0.7×10^3	
	average		6.4×10^4		2.5×10^3	

[a] Heyduk & Lee (1989) *Biochemistry 28*, 6914−6924. [b] Errors in parentheses are expressed in terms of 75% confidence intervals.

the absence of cAMP (*53*). The binding isotherms were analyzed to determine the Adair binding constants in accordance to eq 8. The microscopic binding constants k_1 and k_2 are related to the Adair constants by $K_1 = 2k_1$ and $K_2 = k_1k_2$. Accordingly, the binding affinities of the first and the second cAMP molecules to G141Q are $k_1 = (6.4 \pm 1.3) \times 10^4$ M^{-1} and $k_2 = (2.5 \pm 1.1) \times 10^3$ M^{-1}, respectively, as summarized in Table 1. These values are 2.6 fold higher than that of wild type CRP. However, the ratio of the two constants, k_1/k_2, is identical to that of the wild type, suggesting that the same degree of negative cooperativity exists between the two cAMP binding sites in G141Q as in the wild type protein.

When G141Q was labeled by the fluorescein probe IAF at cysteine 178 in the DNA binding domain, the change in IAF fluorescence can be used for reporting ligand binding to the cAMP binding domain and the response of the DNA binding domain to cAMP binding. It was observed that binding of cAMP to the modified G141Q induces a significant quenching of the fluorescence signal of the fluorescein probe. Hence, the perturbation of the fluorescence intensity of CRP−IAF was employed to measure the binding constant of cAMP to G141Q. Results of cAMP binding are shown in Figure 5. The data were analyzed to determine the binding constants for cAMP. The values of the binding constants derived from this measurement are $k_1 = 1.0 \times 10^5$ M^{-1} and $k_2 = 0.7 \times 10^3$ M^{-1}, as summarized in Table 1. Within the experimental uncertainties these values are in good agreement with those determined by other fluorescence techniques.

Linkage between Subunit Dimerization and cAMP Binding. CRP is a homodimer that undergoes a dynamic association−dissociation reaction between the dimeric and monomeric states. Folded CRP monomer is an intermediate in the CRP folding pathway (*42, 54*). Therefore, in theory, it is possible to determine the equilibrium binding constant of cAMP to the CRP monomer by measuring the apparent binding constants of cAMP to CRP at different protein concentrations. Practically, such a measurement is impossible because the amount of CRP monomer in solution is small and the binding affinity of cAMP to CRP is weak. An alternative approach to solve the problem is to monitor the apparent association constant of the CRP dimer as a function of ligand concentrations. As shown in eq 10, the ratio of the intrinsic and the apparent CRP dimerization constants in the presence of cAMP is a function of K_m, K_{b1}, K_{b2}, and [cAMP]. Since K_{b1} and K_{b2} can be independently determined by cAMP binding assay, K_m can be estimated by measuring $K_a/K_{a,app}$ as a function of cAMP concentration. To overcome the interference of cAMP absorption at the UV region, G141Q

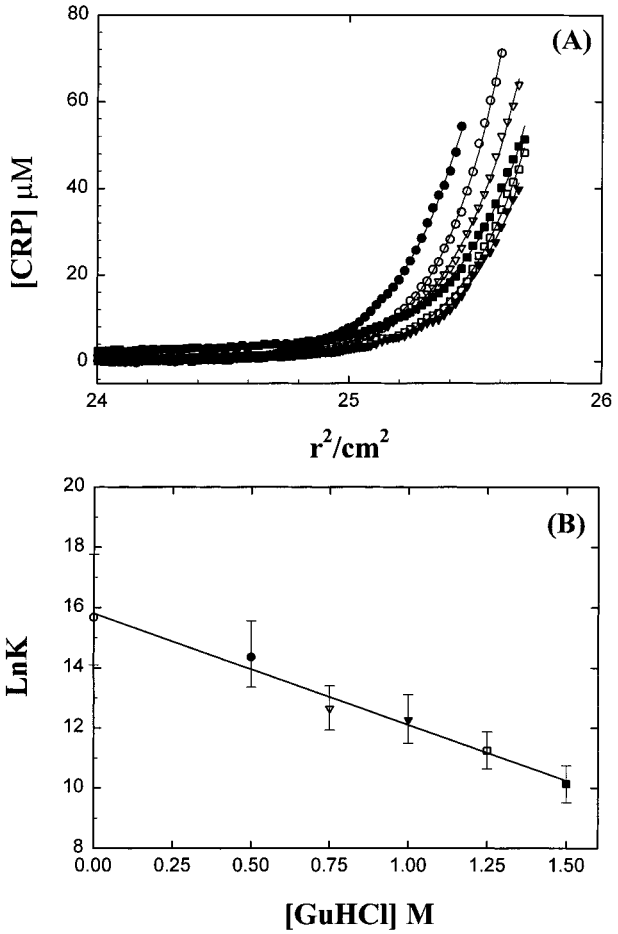

FIGURE 3: Dimer association of G141Q monitored by sedimentation equilibrium as a function of GuHCl concentration. (A) Sedimentation equilibrium profiles of G141Q at different GuHCl concentration; (○) 0, (●) 0.5, (▽) 0.75, (▼) 1.0, (□) 1.25, and (■), 1.5 M GuHCl. The solid lines represent the best fits of the experimental data to eq 1. (B) Apparent dimer equilibrium association constants (determined from A) as a function of GuHCl concentration. The symbols used in B are the same as in A.

was labeled with a fluorescein probe so that the modified protein can be monitored at 495 nm. For each fixed cAMP concentration (0, 19, 574, and 1910 μM), sedimentation equilibrium experiments of the G141Q−IAF complex at three different concentrations of GuHCl (0.5, 1.0, and 1.5 M) were performed to measure the apparent dimer association constant. The apparent dimer association constants of the G141Q−IAF complex in the absence of GuHCl was then determined by extrapolation of the data to zero concentration of GuHCl at each cAMP concentrations. The ratio of K_a/$K_{a.app}$ was plotted as a function of cAMP concentration and compared to the simulated curve derived from calculation using independently determined parameters of K_{b1} (1.28×10^5 M^{-1}), K_{b2} (1.25×10^3 M^{-1}), and hypothetical K_m values ranging from 0 to 2.0×10^5 M^{-1}. From this plot the actual value of K_m can be reasonably estimated as 1×10^4 M^{-1}, as shown in Figure 6.

Conformation of the Subunit Interface Monitored by Proteolytic Digestion. While CRP is resistant to digestion by many proteases in the absence of cAMP, the response of the C-helix of CRP to protease digestion in the presence of cAMP is biphasic (*6*). At low cAMP concentrations (μM) the rate of proteolytic digestion increases as the concentration of cAMP increases. Whereas at high cAMP concentration

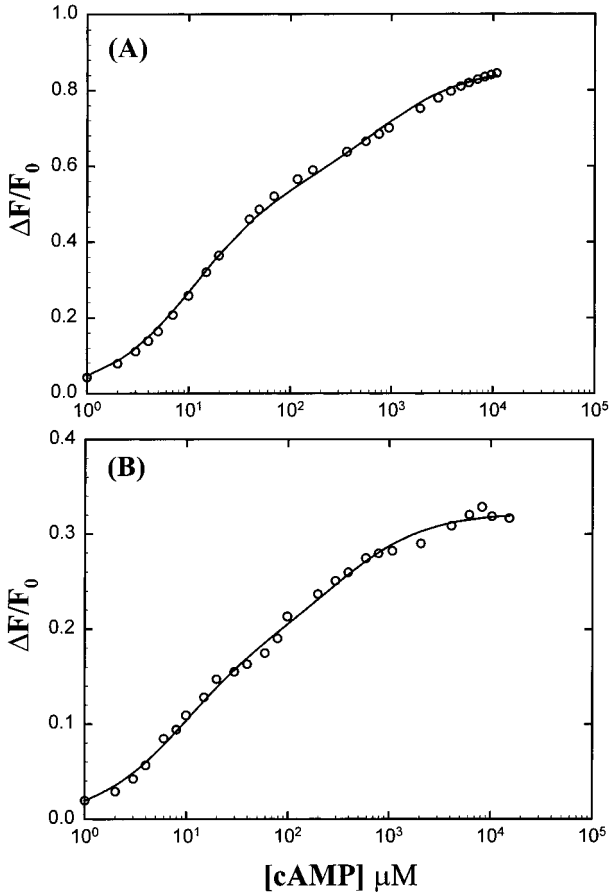

FIGURE 4: Binding of cAMP to the G141Q mutant as monitored by (A) fluorescence of ANS-G141Q complex and (B) intrinsic fluorescence as a function of cAMP concentration. The solid lines represent the best fits of the data to eq 8.

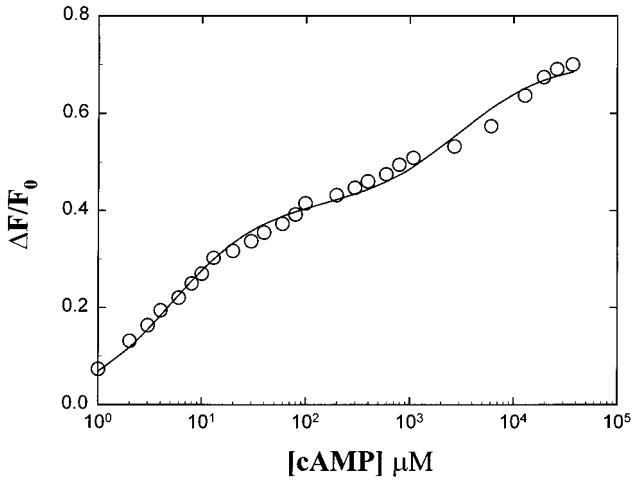

FIGURE 5: Binding of cAMP to the G141Q mutant as monitored by fluorescence quenching of G141Q−IAF complex. The solid lines represent the best fits of the data to eq 8.

(mM) the rate of digestion decreases as the cAMP concentration increases. Therefore, the sensitivity of the C-helix in CRP to protease is a useful probe for monitoring conformational changes along the subunit interface in response to the occupancy of cAMP binding sites.

The sedimentation equilibrium data indicate that the subunit interaction in the G141Q mutant has been perturbed. Proteolytic digestion of the mutant protein was studied to further explore the conformational changes of mutant subunit

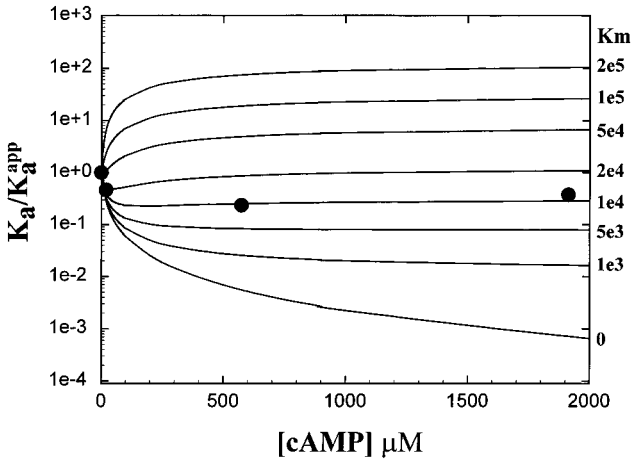

FIGURE 6: Apparent dimer association constant of G141Q as a function of cAMP concentration. The ratio of dimer association constant and apparent dimer association constant determined by sedimentation equilibrium studies of G141Q−IAF is plotted at different cAMP concentrations. The solid lines represent the simulated curves according to eq 10 using different values of K_m as indicated.

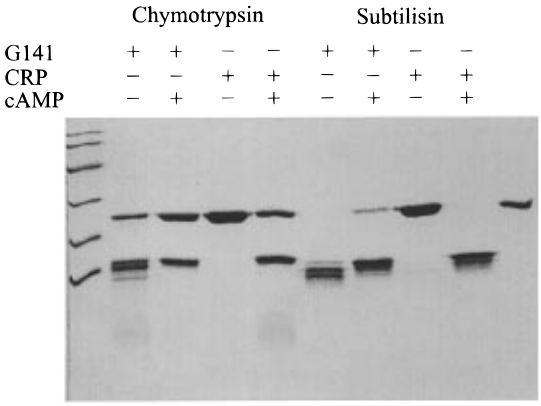

FIGURE 7: Proteolytic digestion of the wild type CRP and G141Q by chymotrypsin and subtilisin in the presence or absence of cAMP. Lanes 1−5 are results with chymotrypsin, while lanes 6−10 are that with subtilisin. Lane 1 is CRP alone; lanes 2 and 3 are with 200 μM and 50 mM cAMP, respectively.

interface. When the susceptibility to chymotrypsin and subtilisin digestion was tested, significantly different results were obtained for the mutant. While the wild type CRP responds to protease digestion in a biphasic manner as a function of cAMP concentrations, mutant G141Q was sensitive to chymotrypsin and subtilisin digestion both in the absence and presence of cAMP. Moreover, the digestion patterns of G141Q in the absence of cAMP by either chymotrypsin or subtilisin were also different from that in the presence of cAMP (Figure 7). These observations indicate that the initial conformation of G141Q is different from that of not only CRP but also the CRP−$cAMP_1$ complex. Additional conformational changes were induced in G141Q upon cAMP binding. It is also clear that the digestion rates of G141Q are dependent on cAMP concentration and decreased with increasing cAMP concentration.

Folding Stability of the Mutant. Protein folding studies in general can provide information on stability of protein molecules and possibly domain−domain interaction in multidomain proteins. The stability of G141Q CRP was monitored by GuHCl denaturation studies using fluorescence

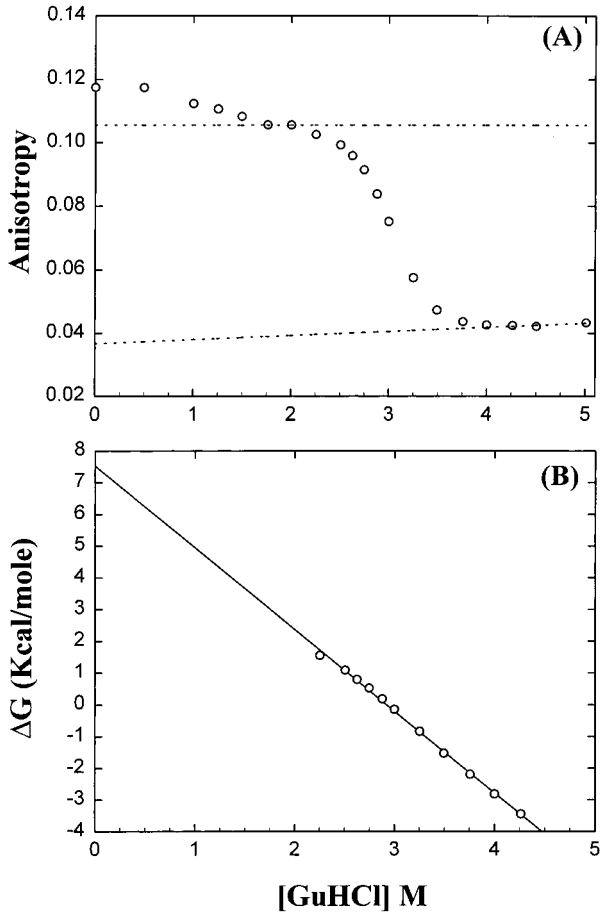

FIGURE 8: GuHCl-induced chemical denaturation of G141Q. (A) Denaturation curve of G141Q (1 μM) measured by fluorescence anisotropy. (B) Apparent unfolding free energy of G141Q monomer as a function of GuHCl concentration.

anistropy to following protein unfolding. The denaturation profile of the G141Q mutant is different from that of the wild type CRP, as shown in Figure 8. The initial decrease of anisotropy at low GuHCl concentrations indicated a dissociation of the G141Q dimer which is consistent with the fact that G141Q has a much larger dissociation constant than that of the wild type CRP. The estimated free energy change for unfolding of the monomeric G141Q is about 7.5 (7.3−7.7) kcal/mol which is close to that of the wild type (*42*). This is consistent with the CD results and Raman spectroscopic study (*51*) that no significant structural change was introduced by a Gly to Gln substitution at residue 141.

DISCUSSION

Some of the most important questions regarding the mechanism of CRP activation by cAMP include: What is the nature of the conformational changes induced by cAMP in CRP and how is the signal of cAMP binding transmitted in the CRP dimer? To address these questions, a strategy is developed, namely, to identify CRP mutants with different phenotypic characteristics and to conduct detailed *in vitro* biophysical measurements to correlate the structural elements perturbed by mutation and the partial reaction(s) involved in the overall DNA−protein interaction perturbed by the specific mutation. The G141Q mutant belongs to the CRP* class, which is able to activate the expression of CRP-dependent operons in a cya^- *E. coli* strain, which lacks

adenylate cyclase, without exogenous cAMP or in the presence of exogenous cGMP *in vivo* (*18, 22*−*28, 55*). It is believed that these CRP* mutants can function in a cAMP-independent manner (*18*−*21, 29*). However, in a previous *in vitro* study from this laboratory it was shown that the G141Q mutant fails to interact with CRP-specific DNA in the absence of cAMP and binding to specific DNA sequence still requires the presence of cAMP. Furthermore, in the presence of many cAMP analogues, G141Q can bind to CRP-specific DNA with relatively high affinity. Some of the natural cyclic nucleotides, such as cGMP and cCMP, can activate G141Q to bind DNA to the extent that is within the affinity range of CRP−$cAMP_1$ for naturally occurring CRP-specific DNA sequences. These results suggest that mutant G141Q not only does not assume an active conformation but also that the activation process is decoupled from its ability to distinguish the specific information embedded in these cyclic nucleotides (*31*).

In this biophysical study, it is established that mutation at residue 141 exerts differential effects on subunit−subunit and domain−domain interactions. The energetics for intersubunit interaction are weakened while interdomain interaction, in general, remains similar to wild type CRP. The correct intersubunit realignment and interdomain rearrangement require the binding of cyclic nucleotide.

The weakening of intersubunit interaction provides an opportunity to probe the behavior of monomeric CRP and to reveal unique features conferred upon dimer formation. The binding of cAMP to monomeric G141Q CRP was monitored through thermodynamic analysis of the linkage between ligand binding and subunit assembly. The linked function relation between cAMP binding (Figures 4 and 5; Table 1) and subunit assembly data (Figure 3) of mutant G141Q can be expressed as

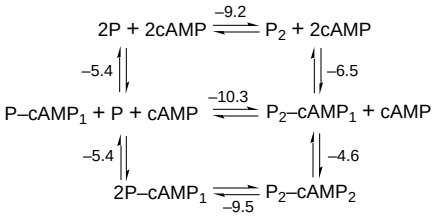

where P and P_2 are monomeric and dimeric CRP, respectively, and the numerical values are ΔG in kcal/mol associated with the reaction for G141Q CRP. The experimentally defined cAMP binding energetics indicate that the total energetics of binding two cAMP molecules to dimeric CRP is −11.1 kcal/mol. Within experimental uncertainties, this value matches that for the formation of two cAMP−monomeric CRP complexes, i.e. $2 \times (-5.4)$ kcal/mol. Interestingly, the energetics of monomeric CRP−$cAMP_1$ formation is between that in loading the first and second site with cAMP in dimeric CRP. Thus, the formation of dimeric CRP leads to a disproportion partition of binding energetics without any portion of the energetics unaccounted for. Knowing the energetics associated with $2P \rightarrow P_2$ and cAMP bindings to monomeric and dimeric CRP, it can be shown that formation of the asymmetric P_2−$cAMP_1$ is favored over the formation of symmetric P_2 or P_2−$cAMP_2$ by approximately 1 kcal/mol. These results indicate that the binding of the first cAMP to P_2 leads to a communication through the subunit interface, the energetic consequence of which is a stronger interfacial interaction. Binding of the second cAMP has to break this favorable interaction and form a new but less energetically favorable interfacial interaction. This is the first evidence for intersubunit interfacial communication upon cAMP binding. Up to date, the evidence to support subunit realignment is the change of accessibility of the C-helix to proteolytic digestion. However, a change in accessibility of digestion sites does not distinguish between the possibilities of perturbation of interfacial interaction upon ligand binding or changes in structural components other than intersubunit interaction that resulted in an exposure or shielding of C-helix from proteolytic digestion.

It is interesting to note that ΔG for $2P \rightarrow P_2$ in wild type CRP is −12 kcal/mol (*42, 54*), a value significantly different from that of G141Q, −9.2 kcal/mol. This difference implies that the subunit alignment in the G141Q mutant is different from that of CRP. This is consistent with the results of proteolytic digestion. G141Q CRP is sensitive to chymotrypsin and subtilisin digestion both in the absence and presence of cAMP whereas wild type CRP is sensitive to protease only in the presence of cAMP.

The effect of G141Q mutation is apparently a differential perturbation on intersubunit interaction without significant consequences in interdomain interaction. The inability of G141Q CRP to bind specific DNA in the absence of cAMP is due, in part, to the failure to assume the appropriate domain rearrangement under those experimental conditions. The implication for domain rearrangement to complete the activation process is supported by two independent sets of results, namely, energetics of unfolding and change in fluorescence signal. The energetics of subunit unfolding have been employed to probe for domain−domain interaction (*42*). It was reported that the free energy change in unfolding CRP, ΔG_u, depends not only on stability of individual domain but also on interaction between the cAMP and DNA binding domains (*42*). Therefore, if the G → Q mutation leads to a perturbation in domain interaction a significant change in ΔG_u may be observed. Unfolding energetics for G141Q CRP is almost identical to that of wild type CRP. Thus, it may be concluded that the interdomain interaction in the ligand free CRP is maintained in the G141Q mutant and the domain rearrangement required for the activation of CRP is not in place in the G141Q mutant in the absence of cyclic nucleotides. This conclusion is consistent with the observation of the change in fluorescence signal of the IAF labeled G141Q CRP in response to cAMP titration. The cAMP binding site in CRP is located in the N-terminal domain while the DNA binding site is in the C-terminal domain. A conformational rearrangement between the cAMP- and DNA-binding domains in response to cAMP binding was monitored by the change in fluorescence intensity of the IAF probe covalently attached to the cysteine 178 residue, which is located at a position just before the DNA-binding helix, F-helix (Figure 1). When the G141Q−IAF complex was titrated with cAMP, a dramatic quenching of fluorescence intensity of the covalently attached fluorescein probe was observed. In addition, the change in the fluorescence signal of the probe reflects quantitatively the binding of cyclic nucleotides to CRP−G141Q. The estimated values of binding constants are in good agreement

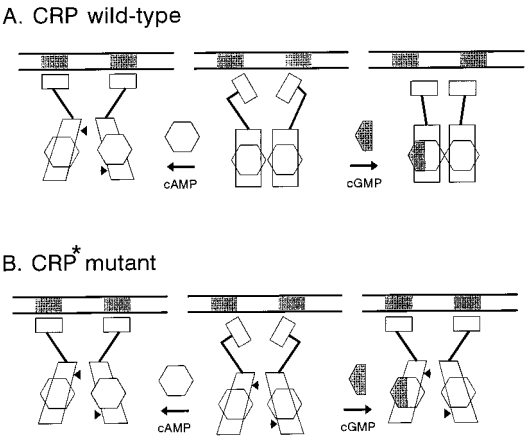

FIGURE 9: Intersubunit and interdomain communication if CRP. (a) Binding of cAMP induces conformational changes which lead to the allosteric activation of the CRP dimer and enable CRP to recognize specific DNA sequences. The minimal functional important conformational changes include coupled subunit realignment and domain reorientation. The subunit realignment induced by cAMP binding allows protease to attack CRP at the C-helix (shown by small arrows). However, cGMP fails to induce proper subunit realignment in CRP; therefore, the CRP−cGMP complex is unable to interact with specific DNA and is also resistant to proteolytic cleavage. (b) In G141Q mutant the subunit architecture is similar to the active CRP−$cAMP_1$ complex. Thus, binding of cAMP and cGMP or other cyclic nucleotides is able to induce further conformational changes required for CRP activation, and G141Q is always sensitive to protease digestion.

with the values determined by other approaches. This again suggests that the cAMP-induced fluorescence quenching is reflecting the intrinsic conformational changes in the DNA-binding domain in response to cAMP binding.

Allosteric activation of CRP requires both proper subunit realignment and domain reorientation. It is evident that mutation G to Q at position 141 leads to an altered subunit interface while the overall domain interactions are maintained. Therefore, G141Q is not in a complete active conformation. Binding of cyclic nucleotides to G141Q presumably can provide the complementary conformational changes, especially proper domain−domain rearrangement, required for activation (Figure 9). On the basis of the CRP crystal structure, this domain−domain rearrangement is most likely a result of the interactions between the cAMP molecule and the β-roll region of the cAMP binding site. Since all the cyclic nucleotides share the common structural elements with cAMP in the interaction with the β-roll portion of the CRP, it is not surprising that once the discriminatory machinery along the subunit interface has been partially disabled by mutation at residue 141, other cyclic nucleotides can produce a domain−domain interaction in mutant CRP similar to that induced by cAMP. In other words, results from this study suggest that CRP maintains its exclusive selectivity for cAMP over other cyclic nucleotides by coupling the intersubunit and interdomain interactions. If this hypothesis were valid, one may predict that mutations capable of decoupling the interfacial interactions, such as G141Q, will lead to a relaxation of cyclic nucleotide selectivity in CRP.

While the interpretation of the data presented is mainly in a model of specific conformational states, as shown in Figure 9, these results are equally consistent with a model that involves a change in the dynamic distribution of an ensemble of microstates of CRP, as proposed earlier (*42*). Additional studies to distinguish these models are in progress. Further studies combining genetic and biophysical measurements of the type presented in this study will be required to complete a structure−function correlation in defining the activation mechanism of CRP. A possibly rewarding approach is to elucidate the effects of mutations at other widely separated parts of the CRP molecule and yet elicit a similar CRP* phenotypic behavior, e.g., the S26F CRP* mutant (*56*). An interesting question is: Do all the CRP* mutants behave the same way? Answer to this question requires similar characterization of more different CRP* mutants. Another intriguing issue is raised by a recent report of Passner and Steitz (*57*) presenting crystallographic evidence of two cAMP binding sites per monomer. One of the sites is located in the C-terminal domain near residue 141. Perhaps one of the future studies should include crystallographic investigations of these CRP mutants to specifically define the effects of mutation on cAMP binding.

ACKNOWLEDGMENT

A critical review of the manuscript by Drs. Hong Pan and John Wooll is appreciated.

REFERENCES

1. de Crombrugghe, B., Busby, S., & Buc, H. (1984) *Science 224*, 831−838.
2. Botsford, J. L., & Harman, J. G. (1992) *Microbiol. Rev. 56*, 100−122.
3. Kolb, A., Busby, S., Buc, H., Garges, S., & Adhya, S. (1993) *Ann. Rev. Biochem. 62*, 749−795.
4. Weber, I. T., & Steitz, T. A. (1987) *J. Mol. Biol. 198*, 311−326.
5. Fried, M., & Crothers, D. M. (1984) *J. Mol. Biol. 172*, 241−262.
6. Heyduk, T., & Lee, J. C. (1989) *Biochemistry 28*, 6914−6924.
7. Heyduk, T., & Lee, J. C. (1990) *Proc. Natl. Acad. Sci. U.S.A. 87*, 1744−1748.
8. Pyles, E. A., & Lee, J. C. (1996) *Biochemistry 35*, 1162−1172.
9. Zinkel, S. S., & Crothers, D. M. (1991) *J. Mol. Biol. 219*, 201−215.
10. Schultz, S. C., Shields, G. C., & Steitz, T. A. (1991) *Science 253*, 1001−1007.
11. Heyduk, E., Heyduk, T., & Lee, J. C. (1992) *Biochemistry 31*, 3682−3688.
12. Ramstein, J., & Lavery, R. (1988) *Proc. Natl. Acad. Sci. U.S.A. 85*, 7231−7235.
13. Lilley, D. M. (1991) *Nature 354*, 359−360.
14. Straney, D. C., Straney, S. B., & Crothers, D. M. (1989) *J. Mol. Biol. 206*, 41−57.
15. Zhou, Y., Busby, S., & Ebright, R. H. (1993) *Cell 73*, 375−379.
16. Zhou, Y., Pendergrast, P. S., Bell, A., Williams, R., Busby, S., & Ebright, R. H. (1994) *EMBO J. 13*, 4549−4557.
17. Heyduk, T., Lee, J. C., Ebright, Y. W., Blatter, E. E., Zhou, Y., & Ebright, R. H. (1993) *Nature 364*, 548−549.
18. Garges, S., & Adhya, S. (1985) *Cell 41*, 745−751.
19. Kim, J., Adhya, S., & Garges, S. (1992) *Proc. Natl. Acad. Sci. U.S.A. 89*, 9700−9704.
20. Ryu, S., Kim, J., Adhya, S., & Garges, S. (1993) *Proc. Natl. Acad. Sci. U.S.A. 90*, 75−79.
21. Sanders, R., & McGeoch, D. (1973) *Proc. Natl. Acad. Sci. U.S.A. 70*, 1017−1021.
22. Takebe, Y., Shibuya, M., & Kaziro, Y. (1978) *J. Biochem. 83*, 1615−1623.
23. Alexander, J. K. (1980) *J. Bacteriol. 144*, 205−209.

24. Melton, T., Snow, L. L., Freitag, C. S.., & Dobrogosz, W. J. (1981) *Mol. Gen. Genet. 182*, 480−489.
25. Harman, J. G., McKenney, K., & Peterkofsky, A. (1986) *J. Biol. Chem. 261*, 16332−16339.
26. Blazy, B., & Ullmann, A. (1986) *J. Biol. Chem. 261*, 11645−11649.
27. Weber, I. T., Gilliland, G. L., Harman, J. G., & Peterkofsky, A. (1987) *J. Biol. Chem. 262*, 5630−5636.
28. Harman, J. G., Peterkofsky, A., & McKenney, K. (1988) *J. Biol. Chem. 263*, 8072−8077.
29. Vaney, M.-C., Gilliland, G. L., Harman, J. G., Peterkofsky, A., & Weber, I. T. (1989) *Biochemistry 28*, 4568−4574.
30. McKay, D. B., Weber, I. T., & Steitz, T. A. (1982) *J. Biol. Chem. 257*, 9518−9524.
31. Cheng, X., & Lee, J. C. (1994) *J. Biol. Chem. 269*, 30781−30784.
32. York, S. S., Lawson, Jr., R. C., & Worah, D. M. (1978) *Biochemistry 17*, 4480−4486.
33. Brickman, E., Soll, L., & Beckwith, J. (1973) *J. Bacteriol. 116*, 582−587.
34. Bernard, H.-U., & Helinski, D. R. (1979) *Methods Enzymol. 68*, 482−492.
35. Gronenborn, A. M., & Clore, G. M. (1982) *Biochemistry 21*, 4040−4048.
36. Takahashi, M., Blazy, B., & Baudras, A. (1980) *Biochemistry 19*, 5124−5130.
37. The Merck Index, 9th ed. (1976) Merck & Co., Inc., Rahway, NJ, p 353.
38. Ferguson, R. N., Edelhoch, H., Saroff, H. A., Robbins, J., & Cahnmann, H. J. (1975) *Biochemistry 14*, 282−289.
39. Sippel, T. O. (1981) *J. Histochem. Cytochem. 29*, 1377−1381.
40. Cheng, X., Kovac, L., & Lee, J. C. (1995) *Biochemistry 34*, 10816−10826.
41. Cheng, X. Ph.D. Dissertation (1994), The University of Texas Medical Branch.
42. Cheng, X., Gonzalez, M., & Lee, J. C. (1993) *Biochemistry 32*, 8130−8139.
43. Yphantis, D. A. (1964) *Biochemistry 3*, 297−317.
44. Aiba, H., Fujimoto, S., & Ozaki, N. (1982) *Nucleic Acids Res. 10*, 1345−1361.
45. Cossart, P., & Gicquel-Sanzey, B. (1982) *Nucleic Acids Res. 10*, 1363−1378.
46. Cohn, E. J., & Edsall, J. T. (1943) in *Proteins, Amino Acids and Peptides* p 372, Van Nostrand-Reinhold, Princeton, NJ.
47. Lee, J. C., & Timasheff, S. N. (1979) *Methods Enzymol. 61*, 49−57.
48. Eftink, M. R. (1997) *Methods Enzymol. 278*, 221−257.
49. Heyduk, E., Heyduk, T., & Lee, J. C. (1992) *J. Biol. Chem. 267*, 3200−3204.
50. Burstein, E. A. (1968) *Biofizika 13*, 433−442.
51. Tan, G.-S., Kelly, P., Kim, J., & Wartell, R. M. (1991) *Biochemistry 30*, 5076−5080.
52. Johnson, M. L., Correia, J. J., Yphantis, D. A., & Halvorson, H. R. (1981) *Biophys. J. 36*, 575−588.
53. Garges, S., & Adhya, S. (1988) *J. Bacteriol. 170*, 1417−1422.
54. Malecki, J., & Wasylewski, Z. (1997) *Eur. J. Biochem. 243*, 660−669.
55. Harman, J. G., & Dobrogosz, W. J. (1983) *J. Bacteriol. 153*, 191−199.
56. Aiba, H., Nakamura, T., Mitani, H., & Mori, H. (1985) *EMBO J. 4*, 3329−3332.
57. Passner, J. M., & Steitz, T. A. (1997) *Proc. Natl. Acad. Sci U.S.A. 94*, 2843−2847.

BI9719455